YMTHE, Volume *27*

Supplemental Information

Short-Term Local Expression of a PD-L1 Blocking Antibody from a Self-Replicating RNA Vector Induces Potent Antitumor Responses

Maria Cristina Ballesteros-Briones, Eva Martisova, Erkuden Casales, Noelia Silva-Pilipich, Maria Buñuales, Javier Galindo, Uxua Mancheño, Marta Gorraiz, Juan J. Lasarte, Grazyna Kochan, David Escors, Alfonso R. Sanchez-Paulete, Ignacio Melero, Jesus Prieto, Ruben Hernandez-Alcoceba, Sandra Hervas-Stubbs, and Cristian Smerdou

Supplementary Materials and methods

Determination of anti-PD-L1 mAb sequence

We first determined the sequences coding for the variable regions of the heavy (HC) and light chain (LC) genes of the anti-PD-L1 mAb produced by hybridoma 10B5, derived from an Armenian hamster immunized with murine PD-L1. [1] Due to the scarce information available for hamster immunoglobulin sequences, we first purified the mAb from the hybridoma supernatant using a protein G-Sepharose column (GE Healthcare Bio-Sciences, Pittsburgh, PA). The purified anti-PD-L1 mAb was digested with trypsin and protein identification was obtained by analysis of the digests in a coupled liquid chromatography and then analyzed by tandem mass spectrometry (LC–MS/MS). This analysis allowed the identification of specific peptides from the constant regions of HC (NH_2-EDTAMYYCAR-COOH) and LC (NH_2-PPSPEELR-COOH) whose sequences were identical to those of available Armenian hamster mAb sequences. [2-3] With this information, specific oligonucleotides were designed for the anti-PD-L1 mAb HC and LC sequences that allowed to reverse transcribe and amplify their mRNAs. Briefly, total RNA was purified from 10B5 hybridoma using the RNeasy kit (Qiagen) and the 5´end of HC and LC mRNAs were reversed transcribed using reverse sense oligonucleotides (for HC: 5´-TCTTGCACAGTAGTACATGG-3´ and for LC: 5´-CCGGAGCTCCTCAGGTGAAG-3´) and amplified by PCR using the 5' RACE System for Rapid Amplification of cDNA Ends (ThermoFisher, Waltham, MA). Since the peptide identifed for HC was in a conserved area within the variable region, the 3´end of its mRNA was also amplified by reverse transcribing total mRNA with a poly-dT oligonucleotide and performing a PCR with the specific forward primer 5´- GAGGACACAGCCATGTACTAC-3´, which sequence was based on the identified HC peptide. In each case, amplified DNA fragments from at least three independent PCR reactions were sequenced, allowing to

determine the nucleotide and amino acid sequences of the variable regions of the anti-PD-L1 LC and HC chains (see next part).

Construction of AAV and SFV vectors expressing anti PD-L1 mAb

A synthetic anti-PD-L1 codon-optimized sequence containing the mAb variable regions described in the previous part and mouse IgG2a and lambda2 constant regions, for HC and LC chains, respectively, was obtained from GenScript (Nanjing, China) cloned in pUC57 flanked by EcoR V sites (pU57-aPDL1). The HC and LC amino acid sequences encoded in this plasmid are the following:

HC: NH_2-MNWGLKLVFFVLILKGVQC**EVQLVESGGGLEQPGKSLKLSCEAS-GFTFSDYYMSWVRQAPGKGLEWVAYISSGSSNIKYVDVVKGRVTISRDNAKNLL SLQMNNLKSEDTAMYYCARGGYALDFWGQGTQVTVSS***AKTTPPSVYPLAPGSAAQ TNSMVTLGCLVKGYFPEPVTVTWNSGSLSSGVHTFPAVLQSDLYTLSSSVTVPSSTWPSETV TCNVAHPASSTKVDKKIVPRDCGCKPCICTVPEVSSVFIFPPKPKDVLTITLTPKVTCVVVDI SKDDPEVQFSWFVDDVEVHTAQTQPREEQFNSTFRSVSELPIMHQDWLNGKEFKCRVNS AAFPAPIEKTISKTKGRPKAPQVYTIPPPKEQMAKDKVSLTCMITDFFPEDITVEWQWNGQ PAENYKNTQPIMDTDGSYFVYSKLNVQKSNWEAGNTFTCSVLHEGLHNHHTEKSLSHSPG K*-COOH

LC: NH_2-AWIPLLLLFFHCTGSFSQ**PLLTQSPSASASLGNSVKITCTLSSQHSTY-GIRWYQQHPDKAPKYVMFVTSDGSHGKGDGIPDRFSGSSSGAHRYLSISNIQSED EADYYCGTGDSTGFVFGSGTQLTVL***GQPKSTPTLTVFPPSSEELKENKATLVCLISNFS PSGVTVAWKANGTPITQGVDTSNPTKEGNKFMASSFLHLTSDQWRSHNSFTCQVTHEGDT VEKSLSPAECL*-COOH

The variable regions of each antiPD-L1 mAb chain are indicated in bold with their signal peptides underlined, while the murine-derived constant regions are indicated in italics.

Plasmid pU57-aPDL1 contained the HC and LC mAb sequences fused by the sequence of 2A autoprotease from foot-and-mouth disease virus (2A), including a furin cleaving site at the carboxyl terminus of the HC, a strategy described earlier for efficient antibody expression [4] (Fig. 1A).

To generate the AAV-aPDL1 plasmid (pAAV-aPDL1), a DNA fragment containing anti-PDL1 mAb sequence was obtained by EcoR V digestion from pUC57-aPDL1 and subcloned under the control of human elongation factor 1 alpha (EF1α) promoter into AAV2 DNA backbone using a pAAV2 plasmid (Agilent Technologies, Sant Clara, CA).

To generate the SFV-aPDL1 vector the anti-PD-L1 mAb sequence was first amplified by PCR from pAAV-aPDL1 with the following primers: Forward: 5´GAGCGGGCCCAATTGGGGACTGAAACTCG3´ and Reverse: 5´GAGCGGGCCCCTA GAGACATTCTGCTGG3´. These primers contained an Apa I site (underlined) which allowed subcloning of the PCR fragment into the Apa I site into pSFVb1-2A [5] in frame with the minimal SFV capsid translation enhancer (b1), using the 2A autoprotease as a linker. Plasmid pSFV-LacZ has been described previously. [6]

Analysis of protein expression by Western Blot

BHK-21 cells were transfected with pAAV-aPDL1 or infected with SFV-aPDL1 (the infectivity of AAV *in vitro* is very inefficient, so the expression of the mAb was analyzed by transfecting the plasmid containing the vector). For transfection, BHK cells were cultured in 6-well plates and incubated with 300 µl of Optimem medium (Invitrogen) containing 2 µg of pAAV-aPDL1 and 5 µl of lipofectamine 2000 (Invitrogen). For infection, confluent BHK cells monolayers were incubated with SFV VPs at a multiplicity of infection of 10 and diluted in 300 µl of MEM medium (Gibco BRL, UK) containing 0.2% bovine serum albumin, 2 mM glutamine and 20 mM Hepes. In both cases (transfection and infection), medium was

removed after 1 h at 37º and cells were incubated for 24h at 37ºC with CHO medium without FBS (Sigma, St. Louis, MO). Supernatants were analysed by Western blot under reducing (with dithiothreitol, DTT) and non-reducing (without DTT) conditions in 12% or 8% polyacrylamide gels, respectively. Anti-PD-L1 mAb was visualized by incubating with a polyclonal goat antibody specific for mouse IgG conjugated with peroxidase (Sigma).

Analysis of mRNA in tumors by RT-qPCR

Tumors were extracted 17h after treatment, homogenized at 4ºC, and total RNA was purified using Maxwell® RSC simplyRNA Cells Kit (Promega, Madison, WI), according to the manufacturer's instructions. DNase I-treated RNA was retrotranscribed to cDNA using random primers (Promega) with M-MLV reverse transcriptase in the presence of RNase OUT (Invitrogen, Carlsbad, CA). For quantitative PCR, cDNAs were amplified using iQ SYBR ® Green Supermix in a C1000 thermal cycler according to the manufacturer's instructions (Bio-Rad, Hercules, CA). cDNAs were amplified with oligonuclotides specific for the following mouse genes: GAPDH (forward: 5´-TGCACCACCAACTGCTTA-3´; reverse: 5´-CAGAAGACTGTGGATGGCCCCTC-3´), 2'-5'-oligoadenylate synthetase 2 (forward: 5´-ACTGTCTGAAGCAGATTGCG-3´; reverse: 5´-TGGAACTGTTGGAAGCAGTC-3´), TRIM-21 (forward: 5´-GCTTCACCTATTCTGTGAGG-3´ ; reverse: 5´-ATCCATTTCCATCTTCTCGG-3´), STAT-I (forward: 5´-TCATCAGTCACCAAGAGAGG -3´ ; reverse: 5´- ATCATTCCAGAGGCACAG -3´), Mx1 (forward: 5´-ATCTGTGCAGGCACTATGAG-3´ ; reverse: 5´- CCTTCCTTCTTTACGCTTCC-3´), and for SFV replicase (forward: 5´-CTGTTCTCGACGCGTCGTC-3´ ; reverse: 5´-GAGGTGTTTCCACGACCC-3´). Relative levels for each RNA were determined with following formula: $2^{\Delta Ct}$ where ΔCt = Ct (GAPDH) – Ct (gene of interest).

Analysis of PD-L1 expression *in vitro*

MC38 and B16-OVA cells were plated in 12-well plates ($5x10^4$ cells/well) and cultured as described during 6h. Then, medium was replaced by new medium containing 100 units/ml of murine IFNγ (Miltenyi, Germany) and incubated for 48h. At that time, cells were collected using diluted trypsin (1:4) and analyzed by flow cytometry as described, using PE-conjugated anti-mouse PD-L1 antibody (Biolegend, clone 10F.9G2).

Supplementary Figure legends

Supplementary Figure S1. Evaluation of antitumor efficacy of SFV-aPDL1 in mice with two MC38 subcutaneous tumors. C57BL/6 mice were inoculated subcutaneously with $5x10^5$ and $3x10^5$ MC38 cells in the lateral and contralateral flanks, respectively. Approximately seven days later (day 0), animals received one intratumoral dose of SFV-aPDL1 ($3x10^8$ VPs) or saline in the lateral tumor (treated), while the contralateral tumor was left untreated. **A**, Evolution of tumor size. Data represent the mean tumor size (mm^2) + SEM. **B**, Survival after treatment. *, $p < 0.05$; ***, $p < 0.001$; ****, $p < 0.0001$.

Supplementary Figure S2. Evaluation of the antitumor effect of SFV-aPDL1 in C57BL/6 mice carrying subcutaneous B16-OVA tumors. $5x10^5$ B16/OVA cells were inoculated subcutaneously into the right flank of C57BL/6 mice and six days later, when tumors had an average diameter of 4-5 mm, animals received one intratumoral dose of $3x10^8$ VPs of the indicated SFV-derived vectors or an equivalent volume of saline. **A**, Evaluation of tumor size (mm^2) for each individual mouse. The fractions in the right corner of each graph indicate the number of complete regressions/total number of mice for each group. **B**, Mean tumor size evolution + SEM. Data are represented only until day 7 since saline mice had to sacrificed at

this time point due to tumor size or ulceration. **C**, Survival after treatment. ***, p <0.001; ****, p <0.0001, ns not significant.

Supplementary Figure S3. Evaluation of SFV-LacZ in combination with anti-PDL1 mAb given IP. C57BL/6 mice bearing subcutaneous tumors were inoculated with SFV-LacZ ($3x10^8$ VPs) IT, with anti-PDL1 mAb (BioXcell. Clon 10F.9G2) given IP as described in Fig. 3, or with a combination of both agents. Mice treated with saline were used as negative control. **A**, Evolution of tumor size (mm^2) along time for each individual mouse. The fractions in the right lower corner of each graph indicate the number of complete regressions/total number of mice in each group. Dashed lines indicate the times of mAb administrations. **B**, Mean tumor size evolution ± SEM. **C**, Survival after treatment. +, p=0.07, *, p <0.05; **, p <0.01; ***, p<0.001****, p<0.0001; ns, not significant.

Supplementary Figure S4. Analysis of PD-L1 expression in tumor cells. (**A**) MC38 and B16-OVA cells were cultured in presence or absence of 100 units/ml of murine IFNγ, incubated for 48h and analyzed by flow cytometry with anti-mouse PD-L1 antibody (n=3). (**B**) C57BL/6 mice bearing subcutaneous MC38 or B16-OVA tumors (n=4-6) were inoculated with the indicated vectors or saline as described in Fig. 5. Five days after treatment tumors were excised, digested and cells were stained for surface marker PD-L1 and analysed by flow cytometry. PD-L1 levels were evaluated in total CD45-negative cells (tumor cells). Histograms to the left of each graph show the expression of PD-L1 on tumor cells as observed in one representative well per condition. **, p <0.01; ****, p<0.0001; ns, not significant.

Supplementary Figure S5. Analysis of CD62L in tumor CD8 T cells. C57BL/6 mice bearing subcutaneous MC38 (**A**) or B16-OVA (**B**) tumors were inoculated with the indicated

vectors or PBS as described in Fig. 5 (MC38) and 7 (B16-OVA). Five days after treatment tumors were excised, digested and freshly purified lymphocytes were stained for surface marker CD62L and analysed by flow cytometry. CD62L levels were evaluated in total CD8 T cells (left graphs) and tumor-specific CD8 T cells ($Tetr^+$) (right graphs). Data represent mean ± SEM (n=6). Asterisks above each bar indicate the statistical comparison of each group with control saline group. Other comparisons are indicated by horizontal bars. *, $p<0.05$; **, $p<0.01$, ns, not significant.

Supplementary Figure S6. Analysis of additional co-stimulatory and co-inhibitory immunological markers in MC38 tumor T cells. Freshly purified lymphocytes were collected from tumors as described in Fig. 5 and analysed by flow cytometry with antibodies specific for the immunological co-stimulatory marker ICOS (**A**), and for immunological co-inhibitory markers TIM3 (**B**) and 2B4 (**C**). Data show levels of each marker in total CD8 cells (left graphs), MC38-specific CD8 T cells (central graphs), and total CD4 T cells (right graphs). Asterisks above bars indicate the statistical comparison of each group with control saline group. Other comparisons are indicated by horizontal bars. *, $p<0.05$; ns, not significant.

Supplementary Figure S7. Analyses of co-stimulatory and co-inhibitory immunological markers on B16-OVA tumor T cells. Tumor-infiltrating lymphocytes obtained as described in Fig. 7 were analyzed by flow cytometry with antibodies specific for the immunological co-inhibitory markers PD-1 (**A**), LAG3 (**B**), and co-stimulatory marker CD137 (**C**). Data show levels (mean ± SEM, n=6) of each marker in total CD8 T cells (left graphs), tumor-specific CD8 T cells (B16-$Tetr^+$, central graphs), and total CD4 T cells (right graphs). Asterisks above

each bar indicate the statistical comparison of each group with control saline group. Other comparisons are indicated by horizontal bars. *, $p<0.05$; ns, not significant.

Supplementary Figure S8. Analyis of CD137 and PD-1 co-expression in MC38 tumors. Tumor-infiltrating lymphocytes were obtained from non-treated MC38 tumors and analyzed by flow cytometry with antibodies specific for PD-1 and CD137. (**A**) The right graph represents the percentage of double positive PD1+ CD137+ in total or tumor specific CD8 cells (MC38 Tetr+). Dot plots show representative gating strategies for the indicated cells. (**B**) Percentage of CD137+ CD8 cells which are PD-1+ or PD-1- (inidcated in the X axis). Data show mean ± SEM, n=6. ****, $p<0.0001$.

Supplementary Figure S9. Gating strategy used to identify CD4 and CD8 T cells in the tumor microenvironment. Lymphocytes were gated from CD45+ cells based on FSC and SSC (**A**). Next, dead cells were removed from the analysis using Zombi NIR fixable dead cell stain (**B**). Doublets were removed from lymphocytes using FSC-A and FSC-H (**C**). Plot in **D** shows CD4+ and CD8+ cell gates and plot in **E** depict Tetramer+ (Tetr) cells in CD8 TILs. Plot Titers refer to the gated population exhibited.

Supplementary References

1. Dong H., Strome S.E., Salomao D.R., Tamura H., Hirano F., Flies D.B. *et al.* (2002). Tumor-associated B7-H1 promotes T-cell apoptosis: a potential mechanism of immune evasion. Nat. Med. 8, 793-800.

2. Verdino P., Witherden D.A., Podshivalova K., Rieder S.E., Havran W.L., Wilson I.A. (2011). cDNA sequence and Fab crystal structure of HL4E10, a hamster IgG lambda light chain antibody stimulatory for gammadelta T cells. PLoS One 6, e19828.

3. Haggart R., Perera J., Huang H.C. (2013). Cloning of a hamster anti-mouse CD79B antibody sequences and identification of a new hamster immunoglobulin lambda constant IGLC gene region. Immunogenetics 65, 473-478.

4. Fang J., Qian J.J., Yi S., Harding T.C., Tu G.H., VanRoey M. *et al.* (2005). Stable antibody expression at therapeutic levels using the 2A peptide. Nat. Biotechnol. 23, 584-590.

5. Rodriguez-Madoz J.R., Prieto J., Smerdou C. (2005). Semliki forest virus vectors engineered to express higher IL-12 levels induce efficient elimination of murine colon adenocarcinomas. Mol. Ther. 12, 153-163.

6. Quetglas J.I., Fioravanti J., Ardaiz N., Medina-Echeverz J., Baraibar I., Prieto J. *et al.* (2012). A Semliki forest virus vector engineered to express IFNalpha induces efficient elimination of established tumors. Gene. Ther. 19, 271-278.

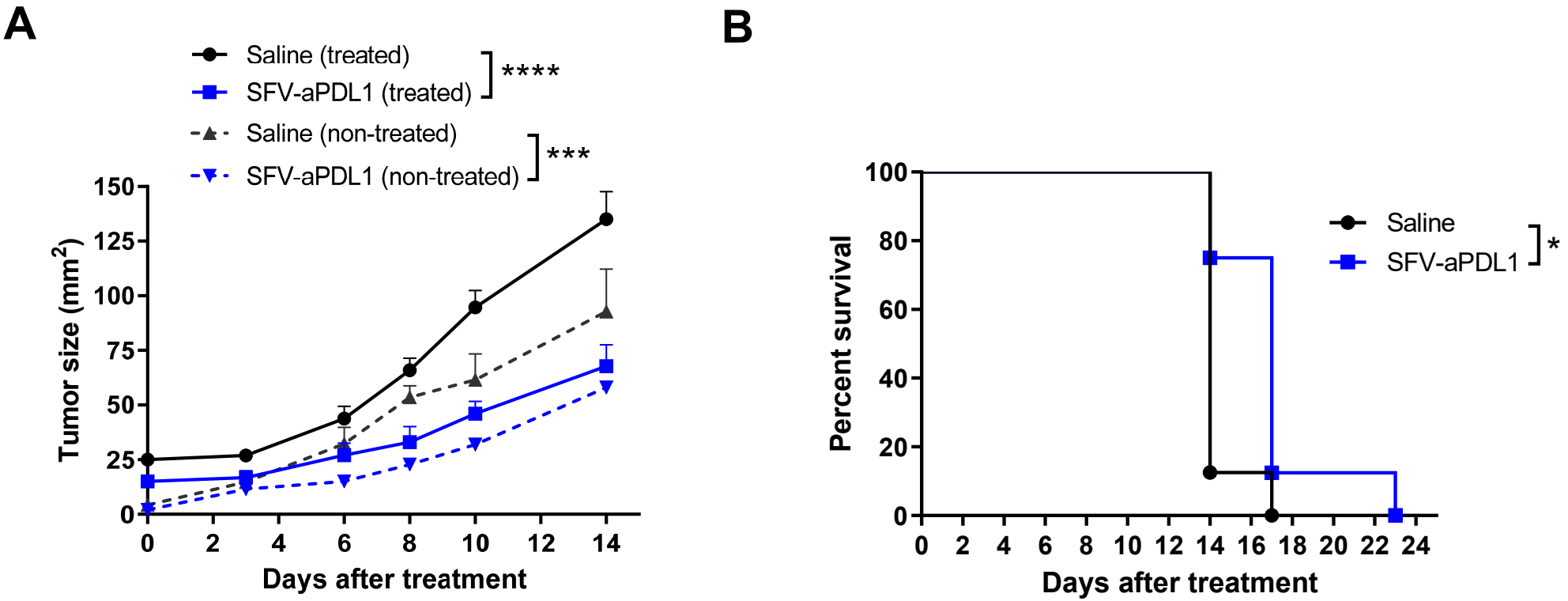

Supplementary Figure S1

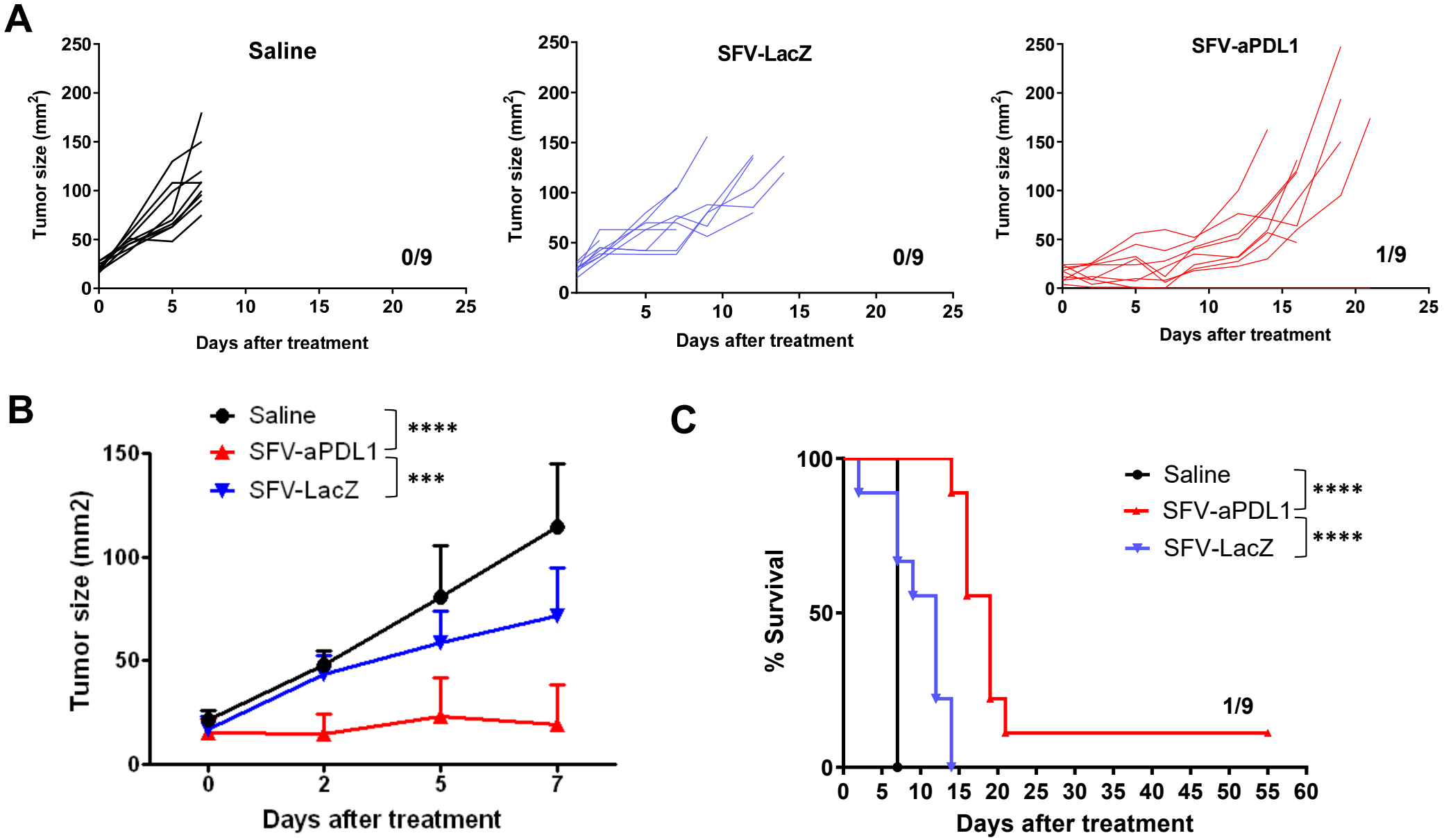

Supplementary Figure S2

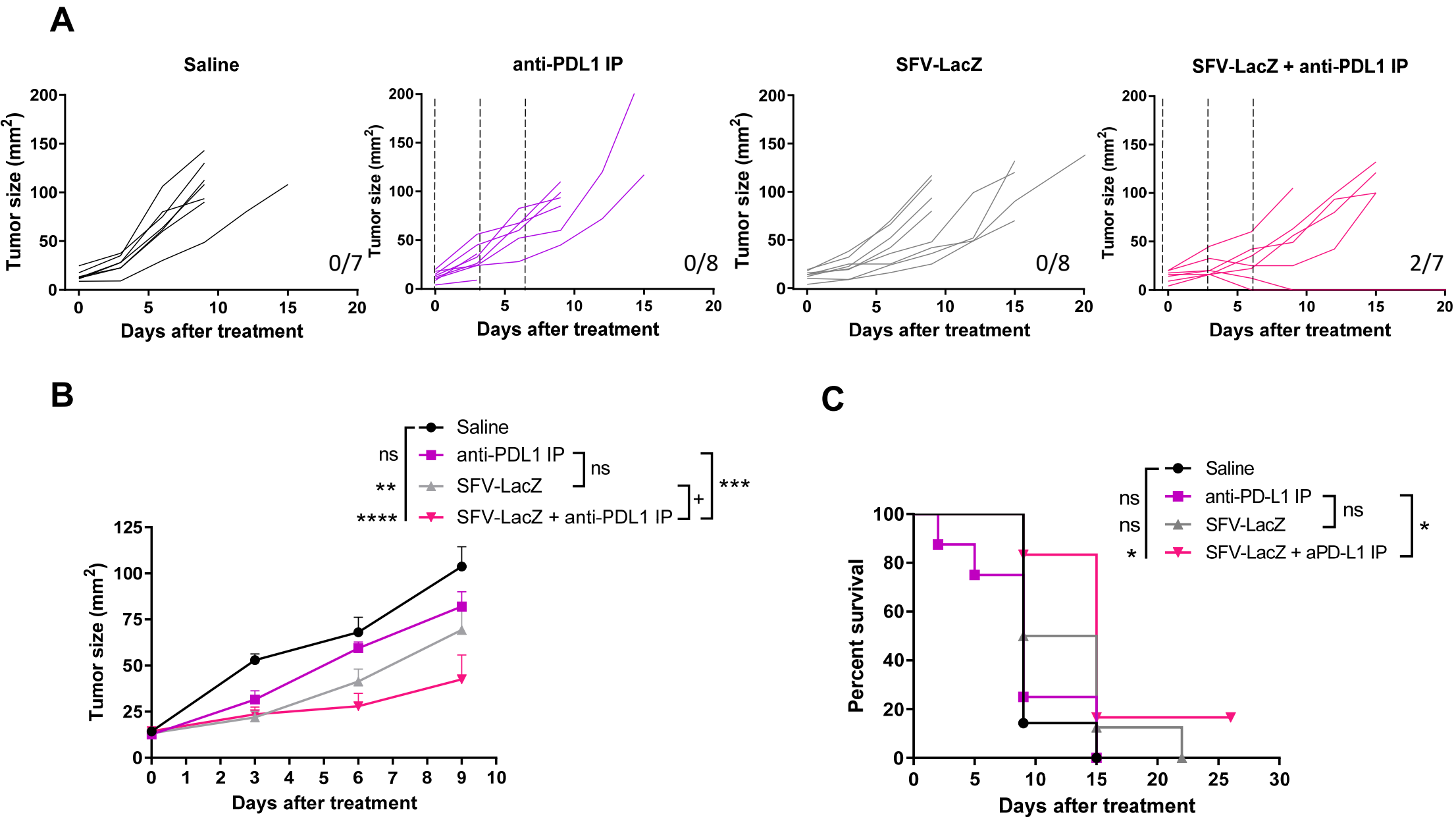

Supplementary Figure S3

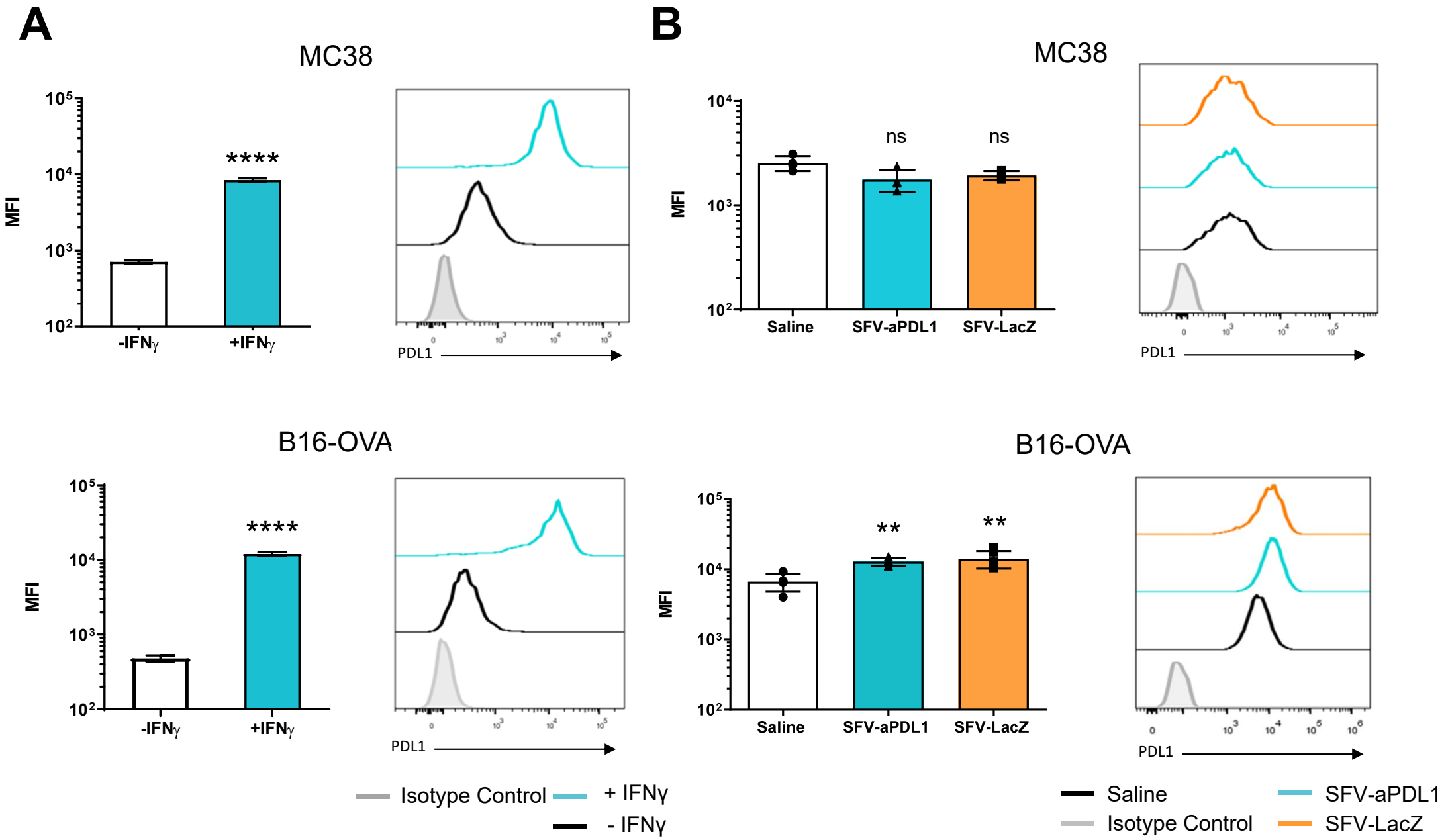

Supplementary Figure S4

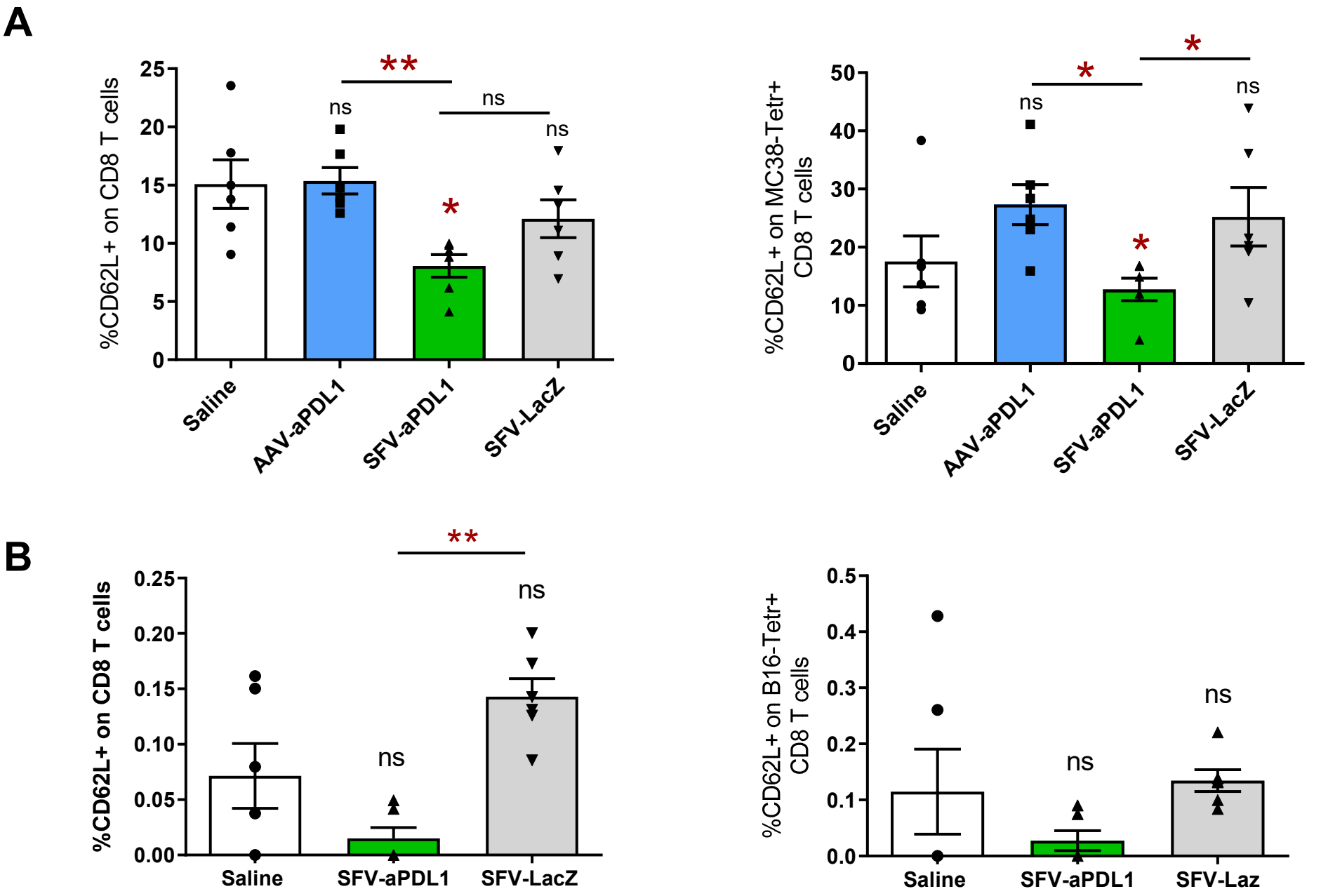

Supplementary Figure S5

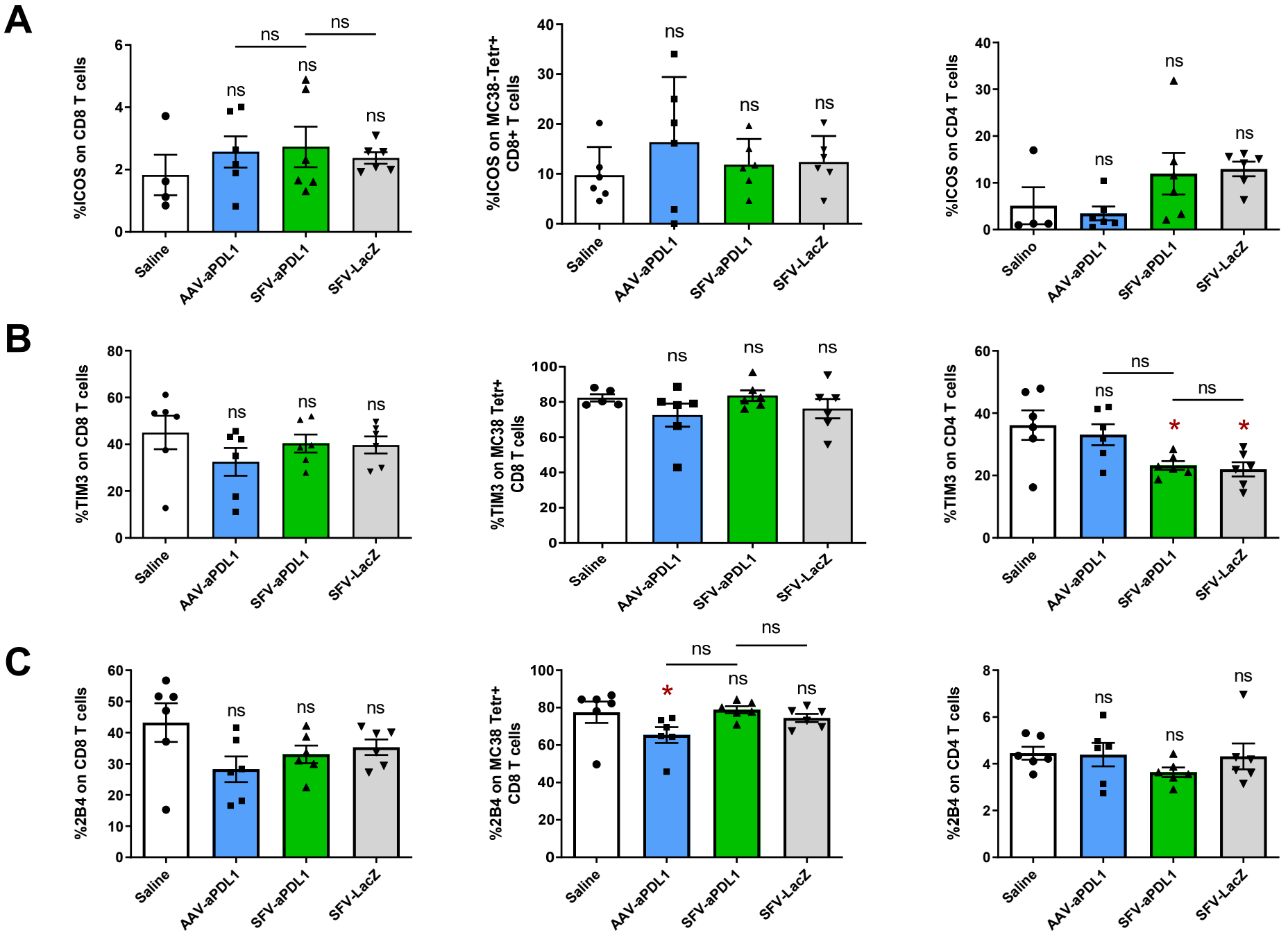

Supplementary Figure S6

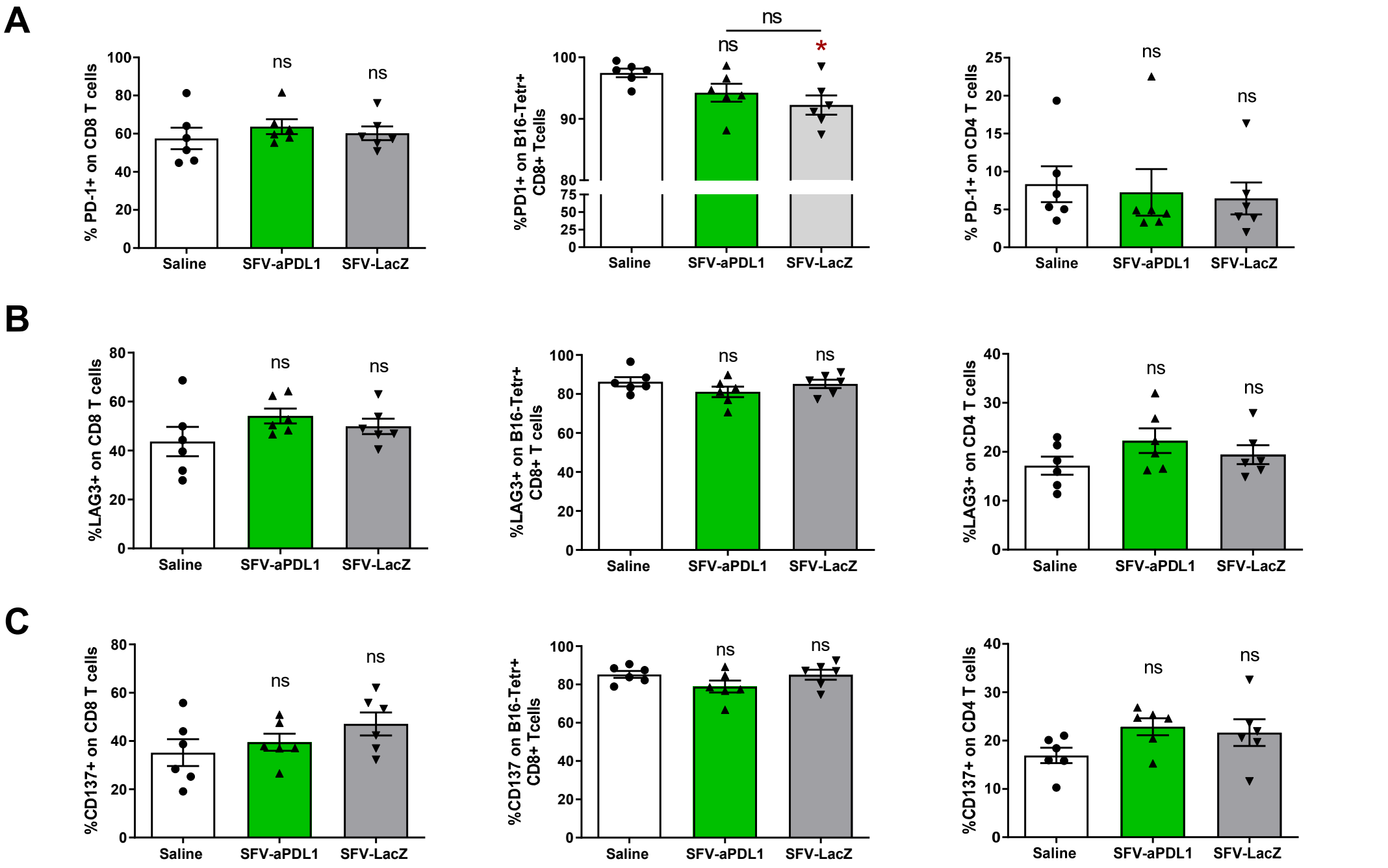

Supplementary Figure S7

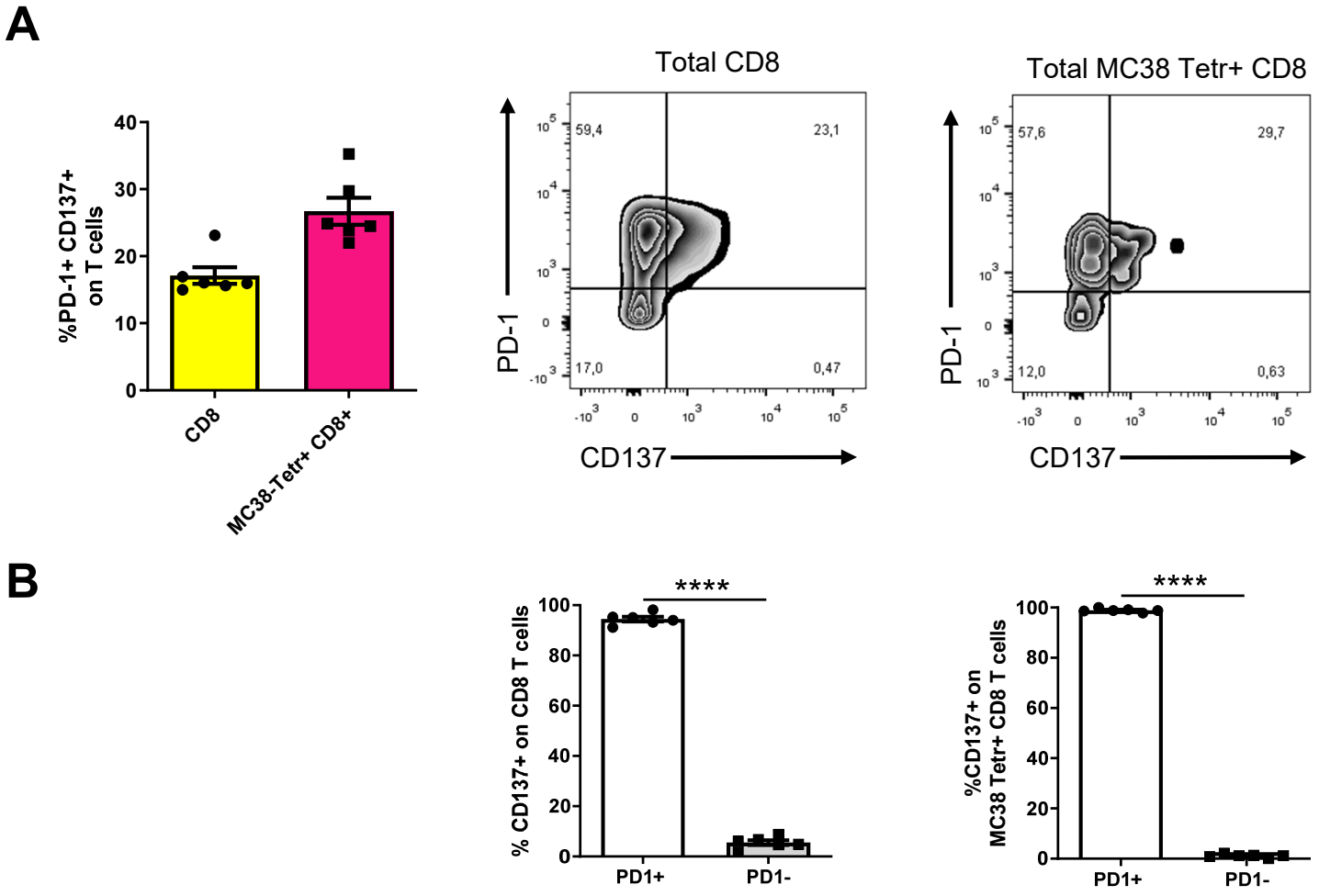

Supplementary Figure S8

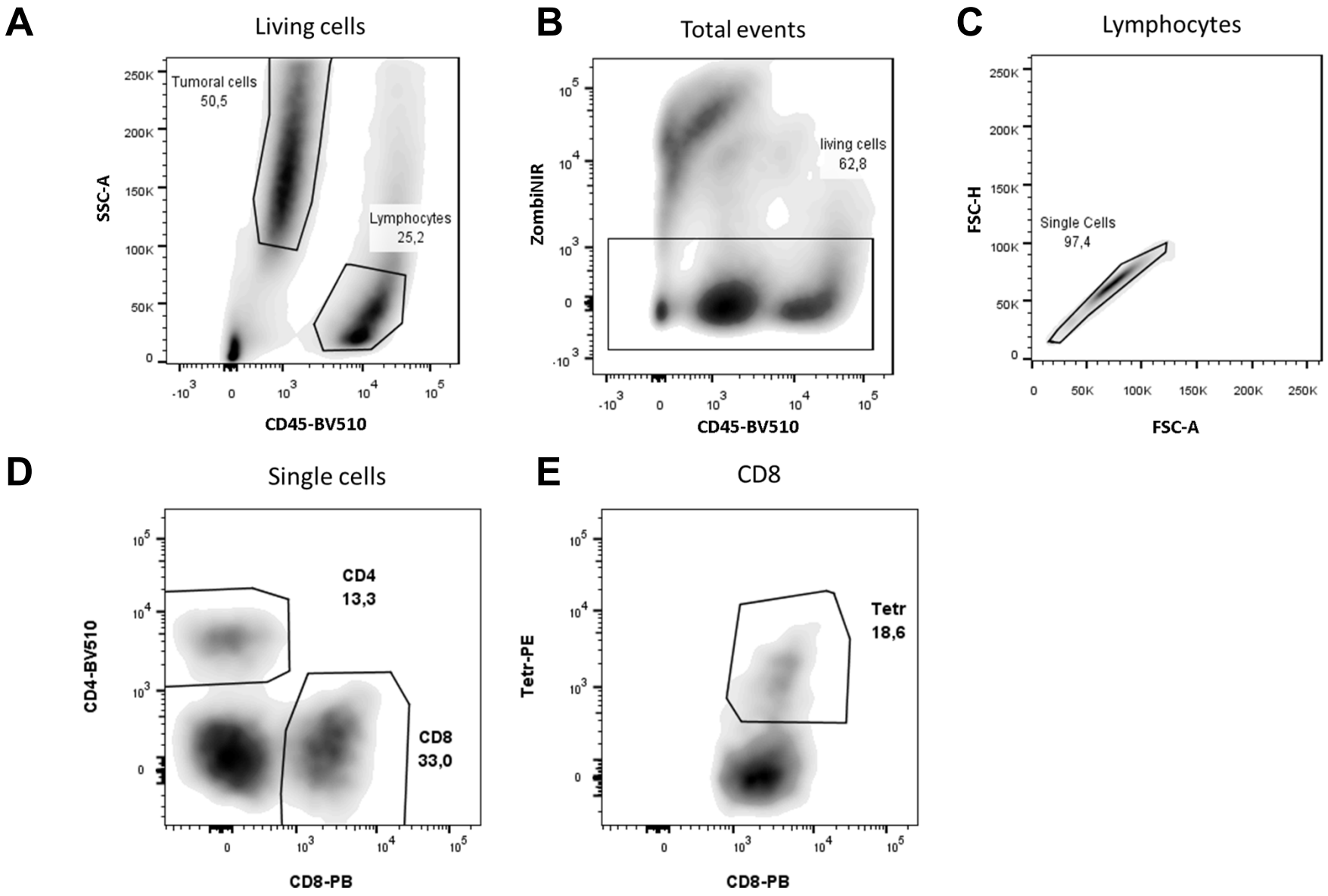

Supplementary Figure S9